BMC Microbiology

RESEARCH

Open Access

Identification of SepF in *Streptococcus suis* involving cell division

Ting Gao[1], Tingting Li[2], Jiajia Zhu[1], Linlin Zheng[2,3], Mo Chen[4], Wei Liu[1], Keli Yang[1], Tengfei Zhang[1], Fangyan Yuan[1], Zewen Liu[1], Rui Guo[1], Chang Li[1], Qiong Wu[1], Yongxiang Tian[1], Rui Zhou[2*] and Danna Zhou[1*]

Abstract

Background *Streptococcus suis* (*S. suis*) is a major zoonotic pathogen that infects humans and pigs. The increasing emergence and dissemination of antibiotic resistance bacteria accelerates the urgent need to develop novel drug targets. Bacterial cell divisome is attractive target. FtsZ, an essential tubulin-like protein, forms a Z-ring that executes the synthesis of the divisome. However, the exact division process of *S. suis* remains unknown.

Results here, we reported a SepF homolog from *S. suis* that modulated the function of FtsZ. *sepF* disruption was not lethal and its deletion mutant (Δ*sepF*) displayed normal growth rate. Δ*sepF* exhibited long chains, occasionally anuclear daughter cells. Electron microscope revealed that the lack of SepF in cells led to abnormal septum which twisted out of shape, and disturbed cell division due to an increased length-width ratio and multiple septal peptidoglycan wall in a cell compared to the wild type strain. Mechanistic studies showed that SepF interacted with FtsZ to promote the bundling of FtsZ protofilaments. Furthermore, sub-cellular localization of FtsZ-GFP in Δ*sepF* also confirmed the abnormal septum and cell morphology.

Conclusions These results showed that SepF was a cell division protein in *S. suis* responsible for maintaining cell shape and regulating FtsZ localization.

Keywords *Streptococcus suis*, Cell division, Septum, Protein-protein interaction, Drug target

Introduction

S. suis (SS) is a major zoonotic pathogen that infects humans and pigs, causing considerable economic losses in the swine industry [1]. *S. suis* infection causes a variety of diseases, such as pneumonia, septicemia, meningitis, and even streptococcal toxic shock-like syndrome [2]. In 1998 and 2005, two large outbreaks of human *S. suis* infection occurred in China, causing 229 infections and 52 deaths [3]. There are 33 serotypes of *S. suis* based on a capsular polysaccharide, among which serotype two (SS2) is considered the most virulent and prevalent strain.

The traditional prevention and treatment of *S. suis* infection depends on vaccination and antibiotics, just like other bacterial infections. However, the complex

*Correspondence:
Rui Zhou
rzhou@mail.hzau.edu.cn
Danna Zhou
zdn66@hbaas.com
[1]Key Laboratory of Prevention and Control Agents for Animal Bacteriosis (Ministry of Agriculture and Rural Affairs), Hubei Provincial Key Laboratory of Animal Pathogenic Microbiology, Institute of Animal Husbandry and Veterinary, Hubei Academy of Agricultural Sciences, Wuhan, China
[2]State Key Laboratory of Agricultural Microbiology, College of Veterinary Medicine, Huazhong Agricultural University, Wuhan, China
[3]Laboratory Animal Center of Shanghai Jiao Tong University, Shanghai, China
[4]College of Animal Science and Technology, Yangtze University, Jingzhou, China

serotypes and diverse sequence types have brought difficulties to clinical treatment through vaccination, because vaccines are unable to provide cross-protection covering all strains [4, 5]. On the other hand, the imprudent use of antibiotics hastens the development of antimicrobial resistance, leading to a severe multidrug-resistant state within *S. suis* [6, 7]. Multidrug resistance testing indicated widespread resistance to macrolides and tetracyclines of *S. suis* strains in different regions of Thailand [8]. While in Spain, *S. suis* isolates showed the greatest resistances for sulphadimethoxine, tetracyclines, neomycin, clindamycin and macrolides [9]. As in China, more than 80% of the *S. suis* isolates were susceptible to penicillin, vancomycin, minocycline and chloramphenicol, and a high frequency of resistance to clindamycin, tetracycline, clarithromycin and erythromycin was also observed [7]. Given the above, the increasing emergence and dissemination of antibiotic resistance bacteria accelerate the urgent need to develop novel drug targets.

Bacterial cell divisome is attractive target, especially in the context of rising multi-drug resistance. FtsZ, a key cell-division protein, self-assembles at the mid-cell region to form a dynamic structure called the Z-ring, then recruits other division proteins to make the cell division septum (the divisome) [10]. The FtsZ assembly and division septum localization is strictly regulated by other division protein. In archaea, positive and negative FtsZ regulators SepF and MinD have been identified [11]. SepF is first reported in *Bacillus subtilis* and plays a role in septum development [12]. In addition, yeast two-hybrid analysis shows that SepF can interact with FtsZ. In *Mycobacterium tuberculosis*, SepF modulates the function of Z-ring, and FtsZ/SepF interaction is a promising drug target for developing agents with novel mechanisms [13].

Although partial function of SepF in other bacterial was documented, the function may be differ in different shaped bacteria. For example, in *Haloferax volcanii*, generating a *sepF* deletion mutant was unsuccessful, suggesting *sepF* deletion was lethal mutant and the role of *sepF* was essential [14]. However, *sepF* mutant affected only the later stages of septum constriction in *Bacillus subtilis* [12], indicating that SepF was not essential in *Bacillus subtilis*. While SepF was not essential in *Mycobacterium tuberculosis* too, since the susceptibility of *sepF* knockdown strain to compound T0349 was increased, which suggested that SepF might be the target of T0349 [13]. Whether SepF can be deleted and the main function of SepF in *S. suis* remains unknown. As is known, *S. suis* is ovococci and can be observed as isolated cells, diplococci, or small chains shaped like elongated ellipsoids. The cell division process in *S. suis* differs great in certain details from that of rod-shaped bacteria (*Bacillus subtilis* and *Mycobacterium tuberculosis*) and archaea (*Haloferax volcanii*) due to its distinct colonization characteristics, pathogenic habitats, and cell wall gene cluster organization [15]. Therefore, research on SepF contributed to cell division in ovococci like zoonotic *S. suis* is of great importance, and can provide the knowledge basis for development of anti-*S. suis* drug.

In this study, we identified a functional gene B9H01_02445, which was annotated as *sepF* in *S. suis* SC19 genome and encoded a cell division protein. Our data demonstrated that *sepF* deletion exhibited long chains, occasionally anuclear daughter cells, abnormal septum and disturbed cell division in *S. suis*. Further mechanistic studies revealed that SepF interacted with FtsZ in vitro and in vivo.

Table 1 Bacterial strains and plasmids used in this study

Strain or plasmid	Characteristics and function[a]	Source or reference
Bacterial strains		
SC19	*S. suis* serotype 2, the wide- type (Strep^r)	(16)
ΔsepF	SC19 *sepF*::*erm* (Strep^r Erm^r)	This study
CΔsepF	SC19 *sepF*::erm/ *sepF*$^+$ (Strep^r Erm^r Spc^r)	This study
E. coli DH5α	Cloning host for recombinant vector	Trans
BL21 (DE3)	Expressing host for fusion protein	Trans
Plasmid		
pAT18	With an Erm^r gene expressing erythromycin resistance rRNA methylase	
pET28a	Expression vector (Kan^r)	Novagen
pSET4s	*E. coli* - *S. suis* Shuttle vector (Spc^r)	
pSET4s-S	Derived from pSET4s for knocking out gene *sepF* in SC19 (Spc^r Erm^r)	This study
pSET2	*E. coli* - *S. suis* Shuttle vector (Spc^r)	
pSET2-S	Derived from pSET2 for functional complementation of sepF (Spc^r)	This study
pSET2-FtsZ-GFP	Derived from pSET2 for FtsZ and GFP fusion expression	This study

Materials and methods

Bacterial strains, media, and growth conditions

The bacterial strains and plasmids used in this study were listed in Table 1. The *S. suis* strain SC19 was isolated from a sick pig during an epidemic outbreak in Sichuan Province in China in 2005 [16]. *S. suis* and its derivatives were cultured in tryptic soy broth (TSB) (BD, Rockville, MD, USA) supplemented with 10% inactivated newborn bovine serum (Sijiqing, Hangzhou, China) at 37℃. Erythromycin (90 μg/mL) was added to screen for the mutant strain. While erythromycin (90 μg/mL) and spectinomycin (100 μg/mL) were added to select for the complemented strain. The *E. coli* DH5α and BL21 strains were grown in LB broth (Difco Laboratories, Franklin Lakes,

NJ, USA) at 37℃. If necessary, kanamycin (25 μg/mL) was added.

Construction of *SepF* gene deletion and complementary strains

All primers used in this study were listed in Table 2 and designed according to the genome sequence of SC19. The *sepF* deletion strain was obtained using homologous recombination method [17]. Primers used in this study were designed according to the genome sequence of *S. suis* strain SC19 (GenBank accession number: CP020863.1). Primers Sup-F/Sup-R and SdownF/Sdown-R were used to amplify the upstream and downstream regions of *sepF*, and the *erm*^{r} expression cassette was amplified from pAT18 using the primers Erm-F/Erm-R. The fragments were cloned into pSET4s to achieve the *sepF*-knockout vector pSET4s-S. Subsequently, the pSET4s-S was electroporated into SC19 and mutant strains were screened as previously described [18]. The complementary strain was constructed by integrating the entire *sepF* coding sequence and its promoter into pSET2 by using primers CF-F/CF-R. The resulting recombinant plasmid pSET2-S was electroporated into strain Δ*sepF* to obtain CΔ*sepF*. To confirm the mutant strain and complementary strain, the *sepF* gene, the upstream, and downstream genes were amplified by PCR using the primer pairs *sepF*-F/ *sepF*-R, 02440-F/02440-R, and 02450-F/02450-R, respectively. Moreover, the resulting DNA fragments were confirmed by DNA sequencing.

Table 2 Primers used in this study

Primers	Primers sequence (5′-3′)	Amplification for
Sup-F	GCGCATGCGTGACCGTTGTGGCTACGGG	Upstream border of *sepF*
Sup-R	GCCTGCAGATTTTCCTCCTCTCCATTAT	
Sdown-F	GCGAGCTCCGCTATGCAAATTTTGATTTT	Downstream border of *sepF*
Sdown-R	GCGAATTCCATTTAGGCGAACTCTCCAT	
Erm-F	AATTTTAGAAAGAAAGATATCTTAGAAGCAAACTTA AGAGTGTGTTGA	Erm^r gene
Erm-R	TTCTTACATGACTTTTGTTCATCGATACAAATTCCCC GTAGG	
SepF-F	TTCTGTTCCAGGGGCCCCTGGGATCCATGGCATTAAA AGATACATTTAAGAACTT	*sepF* gene
SepF-R	AGTCAGTCACGATGCGGCCGCTCGAGTTACCGTTTTA TATCAAATTCAAAATTTG	
CS-F	GCGCATGCCACGCCCTAGACTCTGTCAAA	*sepF* gene and its promoter
CS-R	GCCTGCAGTTACCGTTTTATATCAAATTCAAAAT	
02440-F	ATGAATTTTCAAAAGAATAAGGATGCT	Upstream gene of *sepF*
02440-R	TTATTCAAAGAATGCTGAGCCAATTC	
02450-F	ATGCAAATTTTGATTTTTTTACTATTAAA	Downstream gene of *sepF*
02450-R	CTATGCTAACAGGAGCAA	
FtsZ-F	GTGGACAGCAAATGGGTCGCGGATCCATGG CATTTTCATTTGAAGCAGCAGCTAGTCAT	*ftsZ* gene
FtsZ-R	CAGTGGTGGTGGTGGTGGTGCTCGAGTTAGC GATTACGGAAGAATGGTGGTGTATCCAA	
FtsZg-F	ACTCAAAGGAGAGTAATATAATGGCATTTTC ATTTGAAGC	*ftsZ* gene
FtsZg-R	GGAACTCGATGTCTAGTTTGCGATTACGGAAG AATGG	
GFP-F	CCATTCTTCCGTAATCGCAAACTAGACATCGAG TTCC	GFP gene
GFP-R	AAAACGACGGCCAGTGAATTCTTAGCGATTACG GAAGAAT	

RNA extraction and RT-PCR

To confirm the mutant strain Δ*sepF* and the complementary strain CΔ*sepF*, RT-PCR was performed as previously [19]. Briefly, RNA was isolated using the Bacterial RNA Kit (Omega Bio-Tek, Inc., Norcross, GA, USA) according to the manufacturer's instructions. Then, cDNA was synthesized using the HiScript R II Q Select RT SuperMix for qPCR kit (Vazyme Biotech Co., Ltd., Nanjing, China) according to the manufacturer's instructions. The primers *sepF*-F/*sepF*-R were used to confirm the deletion of *sepF* gene. To confirm whether the upstream and downstream genes of *sepF* were unaffected and functioning normally, the genes were amplified using the primers 02440-F/02440-R and 02450-F/02450-R (Table 2).

Growth characterizations

The growth assay was detected through the measurement of the density changes represented by OD600 nm values and CFU counts of the cultures [18]. SC19, Δ*sepF*, and CΔ*sepF* were grown overnight in TSB medium and then the initial OD600 nm of all subcultures were adjusted to 0.028. The diluted cells were incubated at 180 rpm/m at 37℃ in the same medium. Growth curves were measured by OD600 nm (Victor Nivo, PerkinElmer, Waltham, MA, USA) and CFU counts were taken every hour until the growth process entered stationary phase.

Gram staining

Different strains culture were transferred to the microscope slide respectively, and dried with the heat over a gentle flame. Crystal violet stain was added over the fixed culture. After 10 s, the stain was poured off and rinsed with water. Iodine solution was used to cover the smear for 10 s and rinsed with water. Then, 95% alcohol was added and gently shaken for decolorization. The smear was counterstained with basic fuchsin and rinsed with

water. Lastly, the air-dried smear was undergone a microscopic examination.

Scanning electron microscope and transmission electron microscope observation

The bacterial cell morphology of different strains was examined by transmission electron microscope (TEM) and scanning electron microscope (SEM) as described previously [20]. Briefly, the bacteria cells in the exponential phase were fixed by 2.5% glutaraldehyde at 4 ℃ overnight. Subsequently, the bacterial cells were treated with 1% osmium tetroxide for 2 h at room temperature and dehydrated by series of diluted ethanol. For TEM, the dehydrated bacteria were embedded in epoxy resin and observed by an HT7700 TEM (HITACHI, Tokyo, Japan). For SEM, the dehydrated cells were coated with a 10-nm-thick gold layer for 30 s and analyzed via a SU8100 SEM (HITACHI, Tokyo, Japan).

Structured illumination microscopy observation

HADA is a blue fluorescent D-alanine dye used for labeling of cell wall peptidoglycans in bacteria [21]. Alexa Fluor 647 NHS Ester (AF-647) (Thermo Scientific, Waltham, MA, USA) is a red fluorescent dye used for cell membrane staining. The bacteria cells in the exponential phase mixed with HADA (excitation at 405 nm and emission at 450 nm) at a final concentration of 50 μM, incubated at 37 ℃ for 10 min, then washed thrice with PBS. The resulting resuspension was incubated with AF-647 (excitation at 651 nm and emission at 672 nm) at a final concentration of 20 nM at 37 ℃ for 25 min, then washed thrice with PBS. The image was observed using a structured illumination microscopy (SIM) (Nikon Instruments, Inc., Tokyo, Japan).

The subcellular localization of FtsZ in *S. suis* cells was examined using fluorescently labeled proteins [22]. pSET2-FtsZ-GFP recombinant plasmid was constructed using primers FtsZg-F/FtsZg-R and GFP-F/GFP-R. The Δ*sepF*::pSET2-FtsZ-GFP and SC19:: pSET2-FtsZ-GFP strains expressing the FtsZ -GFP (excitation at 488 nm and emission at 507 nm) fusion protein were cultured in TSB medium at 37 °C to the exponential phase, respectively. The following step staining with HADA and AF-647 was the same as above.

Bacterial two-hybrid assay

Bacterial two-hybrid assay was performed according to the manufacturer's instructions (Euromedex). The genes *sepF* and *ftsZ* were sub-cloned into pUT18 and pKT25 vectors in frame with the open reading frames, respectively. The two recombinant plasmids either pUT18-SepF and pKT25-FtsZ, or pUT18-FtsZ and pKT25-SepF were co-transformed into competent BTH101 reporter cells. pUT18-Zip and pKT25-Zip were co-transformed as positive control, while pUT18 and pKT25 were co-transformed as negative control. Transformants were plated on indicator plates containing ampicillin (100 mg/mL), kanamycin (50 mg/mL), IPTG (0.5 mM), and X-gal (40 mg/mL), then incubated at 30 °C overnight and the results were documented.

Protein expression

The genes *sepF* and *ftsZ* were sub-cloned into PGEX-6p-1 and pET28a vectors in frame with the open reading frames, respectively. The recombinant plasmids were transformed into *E. coli* BL21. The resulting BL21 cultured to OD600 nm reached 0.6 were induced with 0.1 mM isopropyl β-d-thiogalactopyranoside (IPTG) and cultured in Luria broth at 37 °C for 4 h. BL21 were then harvested, sonicated in cold PBS, and purified with Glutathione S-transferase (GenScript, Nanjing, China) beads or Nickel-nitrilotriacetic acid (GenScript, Nanjing, China) beads according to the users' manual. Efficiency of purification was verified by SDS-PAGE, followed by Coomassie blue staining.

GST (glutathione S-transferase) pull-down assays

For GST pull-down assays [23], an equal amount (0.5 mg) of GST-SepF fusion protein and His-FtsZ fusion protein were mixed and incubated on ice for 3 h. Subsequently, the mixture was loaded onto Glutathione Sepharose 4B resin columns. After being washed five times with wash buffer (Tris-HCl 50mM, NaCl 150mM, glycerin 10%, sucrose 10mM, EDTA 5mM, TritonX-100 0.1%), proteins were eluted with wash buffer supplemented with 15 mM reduced glutathione. The eluates were separated using 12% SDS-PAGE, transferred to PVDF membranes (Millipore, Billerica, MA, USA), and probed with anti-His antibody (Sigma-Aldrich, Merck KGaA, Darmstadt, Germany). GST and His6 from Wuhan Genecreate (Wuhan, China) were used as negative controls. There were three replications for each pull-down assay.

Bio-layer interferometry analysis

The binding kinetics of SepF and FtsZ was monitored using a bio-layer interferometry instrument (ForteBio, CA, USA) [24]. SepF was labeled with biotin through biotin labeling kit (LinKine, Wuhan, China), diluted to 50 nM and immobilized on the streptavidin (SA) biosensors. The protein FtsZ at 1 mg/mL underwent two doubling dilutions in PBS. First, the sensors were pre-wetted in PBST (PBS containing 0.02% (v/v) Tween20) for 300 s. Then, association between SepF and FtsZ was conducted for 300 s, and dissociation was performed in PBST for 600 s. The data were analyzed using the DataAnalysisHT ForteBio Octet analysis software (ForteBio, Menlo Park, CA).

FtsZ polymerization assay

The effect of SepF on FtsZ polymerization was visualized by transmission electron microscopy as previous described [25]. The polymerization reaction of 50 μL was set with a final concentration of 6 μM SepF, 6 μM FtsZ, 1 μM GTP and 10 mM $MgCl_2$ at 30 °C for 15 min. After incubation, the reaction mixture was deposited onto a 400-mesh glow-discharged Formvar carbon-coated copper grid for 10 min. The grids were then added 5% (w/v) uranyl acetate, air-dried, and subjected to observation the images of the filaments under TEM.

Statistical analyses

Cell length and width of bacteria were measured with ImageJ software. Unless otherwise specified, statistical analyses were performed via unpaired Student's *t*-tests in GraphPad Prism 8 software (GraphPad Software, CA, USA). A *p*-value of less than 0.05 was considered statistically significant. All experiments were performed in triplicate at least three times.

Results

Confirmation and growth characterization of Δ*sepF* and CΔ*sepF*

PCR and RT-PCR were conducted to confirm the mutant strain Δ*sepF* and complementary CΔ*sepF*. As shown in Fig. 1, *sepF* expressed in SC19 and CΔ*sepF*, but not in strain Δ*sepF* at the DNA and RNA levels (Fig. 1A). Further, the transcripts of *sepF* upstream and downstream genes were not affected by the deletion (Fig. 1B and Fig. S1), which could exclude associated polarity effects. To characterize SC19, Δ*sepF* and CΔ*sepF*, the bacterial growth was detected by OD600 nm and CFU counts. Interestingly, the Δ*sepF* strain showed a similar growth trend to that of SC19 strain, although the values of OD600 nm and CFU counts slightly decreased at the exponential phase (Fig. 1C-D).

SepF affects bacterial morphology and septum localization

The effect of *sepF* knockout on morphology of *S. suis* was investigated using Gram staining, SEM, TEM and

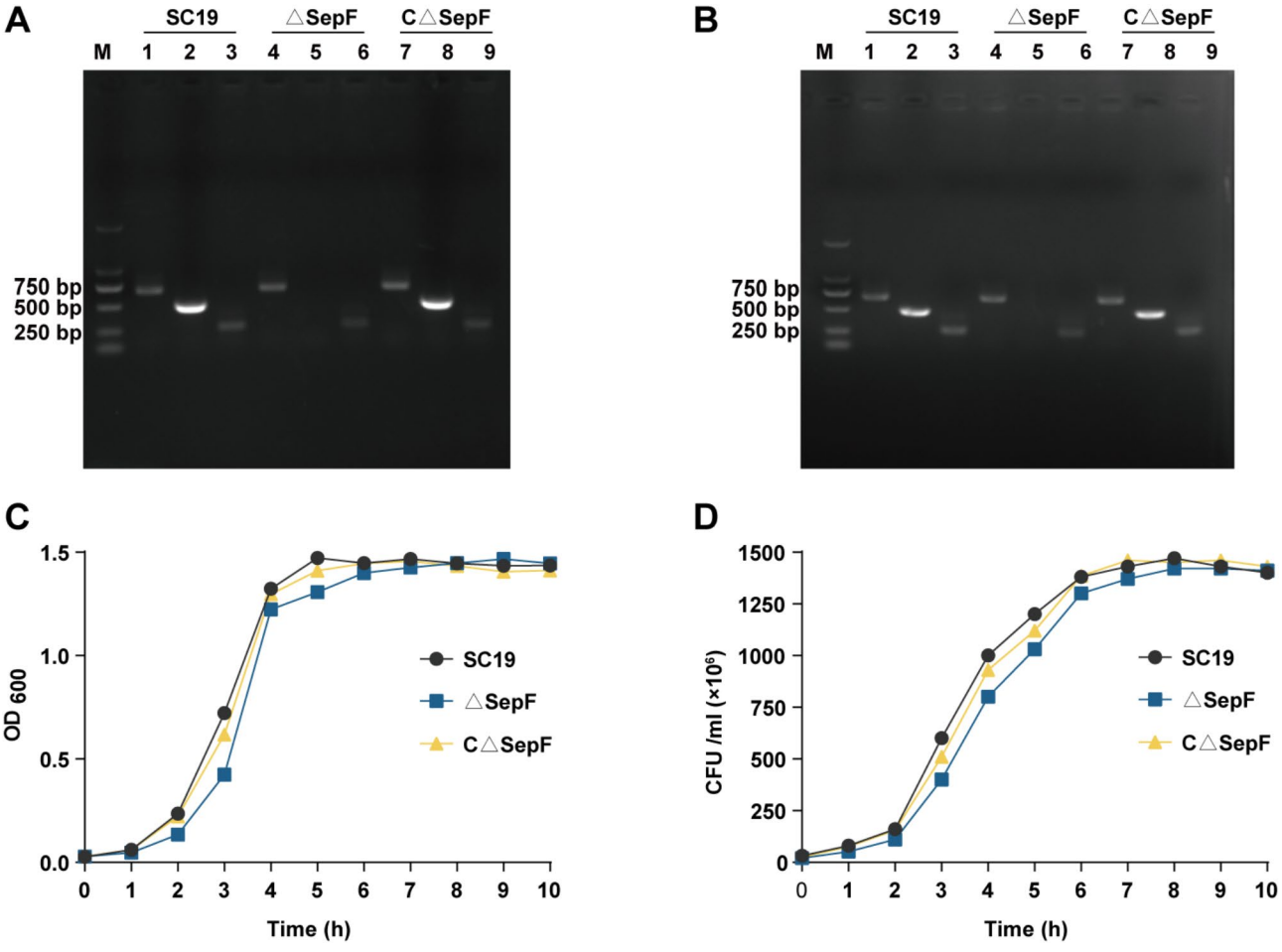

Fig. 1 Construction and characterization of Δ*sepF* and CΔ*sepF*. **A**: DNA level of the *sepF* gene, the upstream, and downstream genes in SC19, Δ*sepF* and CΔ*sepF*; **B**: Transcription levels of the *sepF* gene, the upstream, and downstream genes in SC19, Δ*sepF* and CΔ*sepF*; **C**: The growth curve of SC19, Δ*sepF* and CΔ*sepF* measured by OD600 nm; D: The growth curve of SC19, Δ*sepF* and CΔ*sepF* measured by CFU counts

SIM (Fig. 2). The results revealed that *sepF* deletion triggered significant chain elongation. Almost 200 bacterial cells were randomly chosen from the TEM and SIM micrographs to measure the chain length, cell length and cell width. Compared with the SC19 that displayed a short chain length with less than 5 cells (82%), 26% of Δ*sepF* showed a chain length between 5 and 10 cells, and 49% of Δ*sepF* showed a chain length more than 10 cells (Fig. 2A), suggesting the low degree of cell separation of the mutant cells. In addition, the cell length was significantly longer in Δ*sepF* (1.378 ± 0.03032 μm) than in SC19 (1.284 ± 0.01958 μm; $p < 0.05$;), while the cell width displayed no significant difference among the three strains, leading to an increased length-width ratio in Δ*sepF* (Fig. 2B-D). These results indicated that SepF played a vital role in maintaining bacterial morphology.

Furthermore, in 16.0% (39/243) of the Δ*sepF* cells, the septum was not localized in the mid-cell, especially the angles of the septum were not vertical to the cell long axis as the SC19, resulting in the formation of twisted cell chains (Figs. 2A and 3; pointed by red and white arrows). About 9.1% (22/243) of the Δ*sepF* cells displayed disordered division, leading to the formation of unequal-sized daughter cells, meanwhile 7.8% (19/243) formed elongated cells containing multiple and un-constricted cell division rings (Figs. 2A and 3) (pointed by red and white arrows). Consequently, the absence of SepF disturbed proper septum localization and construction, in turn affecting the capability of mutant cells to effectively divide.

SepF interacts with division protein FtsZ

To reveal the underline mechanism of SepF on cell division, protein-protein interaction was analyzed by bacterial two-hybrid, GST pull-down assays, and BLI assay. The fusion strains containing full-length *sepF* and *ftsZ* grew well on the indicator plates with a blue color, whereas the negative control did not grow (Fig. 4A). Bacterial two-hybrid system is a simple and fast approach to detect protein-protein interaction in vivo. Subsequently, protein-protein interaction in vitro was carried out. GST pull-down experiments further corroborated the direct binding between SepF and FtsZ (Fig. 4B). The input channels were used as positive control. In the pull-down experiment, the his-tag was detected in the tested channel not in the control channel, suggesting that SepF could combine with FtsZ. The original western blot image was shown in Fig. S2. Moreover, BLI assay was used to monitor the binding kinetics of SepF and FtsZ. As shown in the association and dissociation kinetic chart (Fig. 4C), the affinity of SepF to FtsZ increased in a dose-dependent manner, FtsZ was rapidly bound to but slowly dissociated from SA-biosensors coated with SepF. The KD value for the binding was 0.67 nM. These data suggested that SepF interacted with FtsZ both in vivo and in vitro.

SepF enhances FtsZ polymerization into protofilament

TEM was carried out to investigate the morphological change of FtsZ protein during protofilament formation. FtsZ assembled into polymers in the presence of GTP (Fig. 4D) (black spots pointed by red arrows). After incubating FtsZ with SepF in the presence of GTP, the FtsZ formed into long protofilament (Fig. 4D) (black spots pointed by red arrows), revealing that SepF directly promoted the formation of FtsZ protofilament in vitro.

SepF affects septum localization through interaction with FtsZ

To gain an insight into the interaction between SepF and FtsZ under physiological conditions and the influence of SepF on subcellular localization of FtsZ, a green fluorescent protein -tagged FtsZ (GFP- FtsZ) was expressed in SC19 and Δ*sepF* strains, respectively, and observed by SIM. GFP- FtsZ was found at the mid-cell of SC19 as shown in Fig. 5, this was consistent with previous report [26]. GFP-tagged FtsZ, AF647 and HADA staining revealed that compared to SC19 formed a typical ovoid shape, *sepF* deletion caused severe cell division defects, generating longer bacterial cell, abnormal localization of the interacting protein FtsZ, which in turn leading to disordered Z-ring septum that was organized into multiple and un-constricted cell division rings. These results indicated that interaction between SepF and FtsZ was vital for septum localization and normal cell division, furthermore, SepF could align Z-ring during cell division.

Discussion

In almost all bacteria, the filamenting temperature-sensitive cell division protein FtsZ polymerizes to form a Z-ring that marks the site of division septum, then recruits other proteins to compose the divisome [27]. Since the divisome is essential in bacterial proliferation, it becomes attractive target for novel drug discovery. The Z-ring septum localization is strictly modulated by related cell division proteins. Until now, more than 30 proteins are proven or likely to function in the pneumococcal division process [28]. However, Z-ring septum precise localization, then leading to one parent cell becomes two symmetrical daughter cells, resulting in normal ovoid-shaped *S. suis* with short chain length remains largely unknown. A few of regulatory proteins have been found to be intimately related to cell division and ovococci morphogenesis in *S. suis*, such as DivIVA, playing diverse roles in division site selection, chromosome segregation and controlling peptidoglycan homeostasis [29]; STK, an eukaryote-like serine/threonine kinase; Msmk, an ATPase that contributes to the transport of multiple

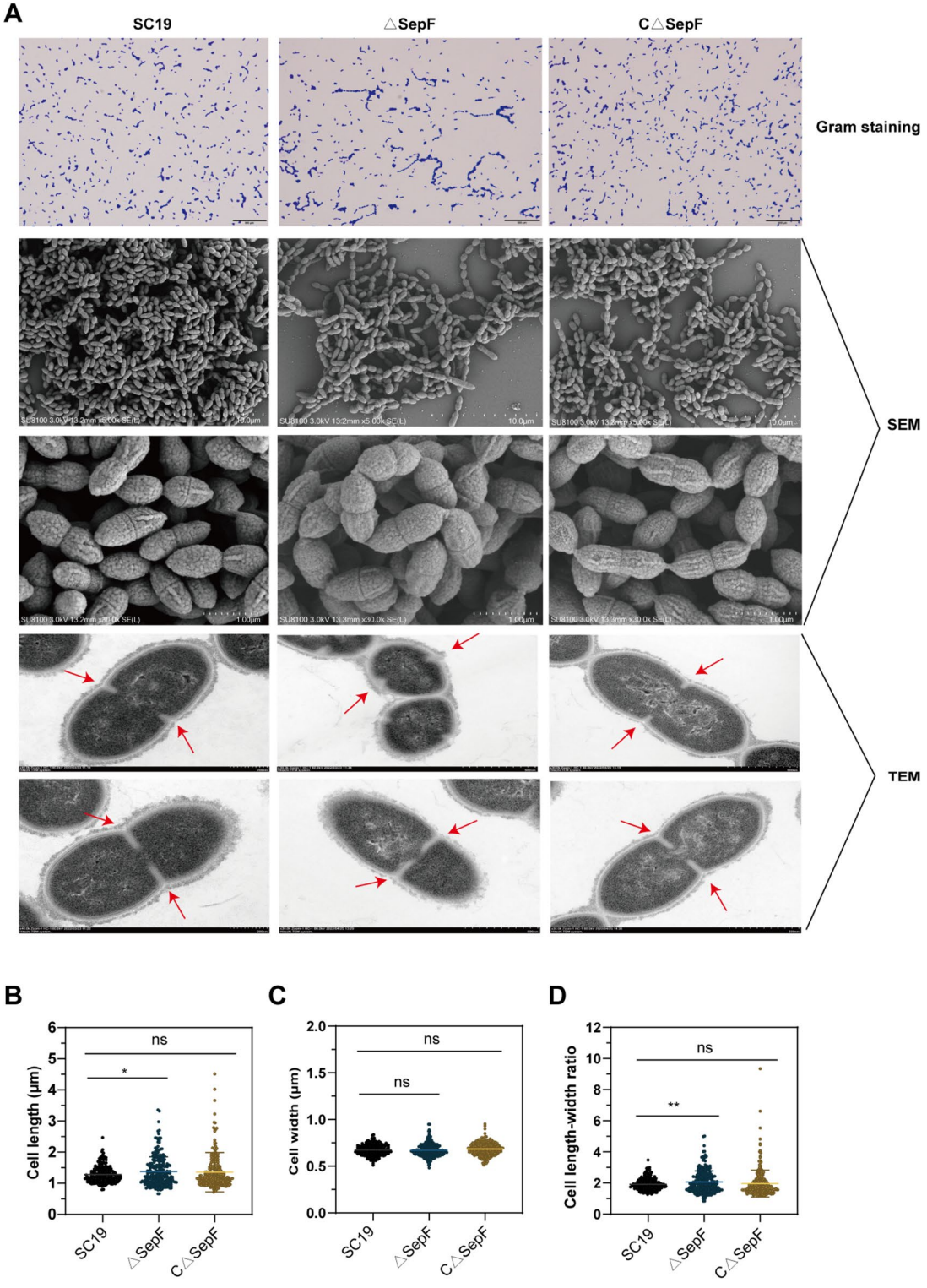

Fig. 2 Morphological analysis of the SC19 and Δ*sepF* strains. **A**: Gram staining (The scale bar is 500 μm), scanning electron microscope (The scale bar is 10 μm–1 μm) and transmission electron microscope (The scale bar is 200–500 μm) images of SC19 and Δ*sepF* strains; **B**: Cell length of SC19, Δ*sepF* and CΔ*sepF* strains; **C**: Cell width of SC19, Δ*sepF* and CΔ*sepF* strains; **D**: Cell length-width ratio of SC19, Δ*sepF* and CΔ*sepF* strains. The results of cell length and cell width were obtained by measuring at least 200 bacterial cells per sample. The height of the bars indicates the mean values for the relative expression data ± SEM (*, $p < 0.05$; **, $p < 0.01$; ns, $p > 0.05$)

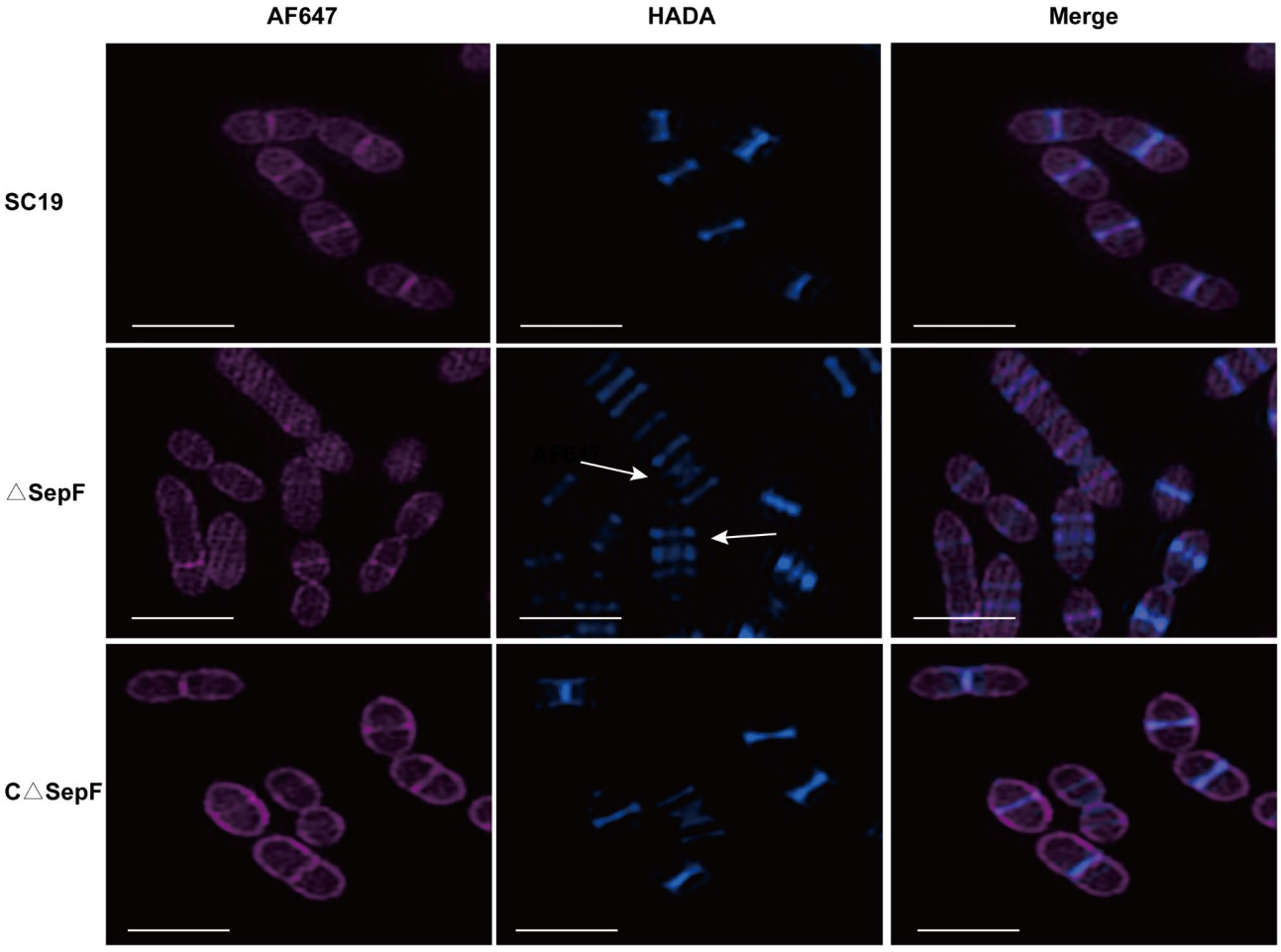

Fig. 3 Structured illumination microscopy analysis of SC19, Δ*sepF* and CΔ*sepF* strains. The mid-log phase bacterial cells were stained with AF-647 (red fluorescence) and HADA (blue fluorescence) dyes, followed by imaging with SIM. The scale bars are 2 μm

carbohydrates [15, 30]. In this study, a SepF homolog of the zoonotic *S. suis* was identified. SepF was also connected to cell division and ovococci morphogenesis, which was consistent with previous report [11, 13].

In the growth assay, we found that gene *sepF* deletion nearly had no impact on the CFU counting and OD600 nm of SC19. Whereas, it was noticed that the morphological characteristics of Δ*sepF* differed from SC19 observed through TEM, SEM and SIM (Figs. 1, 2 and 3). In the previous study, peptidoglycan synthesis related protein DivIVA deletion lead to a low growth rate in SC19 and serine/threonine kinase STK knock-out displayed no significant difference in OD600 nm, but reduced CFU counting. As mentioned above, SepF, DivIVA and STK had no influence on growth tested by OD600 nm, however, the three mutant strains exhibited significant chain elongation in common. This phenotype may be on account of the differences in the light-scattering properties of normal and filamentous cocci [31]. Although SepF nearly had no impact on growth rate, its deletion markedly decreased the virulence of SC19 (Fig. S3-4).

So far, the *sepF* gene is essential to *Haloferax volcanii*, but can be deleted in *Bacillus subtilis* and *Mycobacterium tuberculosis*. In this study, we confirmed that SepF deletion was not lethal mutation in *S. suis*, since *sepF* mutant was viable, and lead to an increased length-width ratio and abnormal septum (Figs. 2 and 3). Because, cell division systems are much less uniform in different bacteria, and different shaped bacteria exhibit different division mode. Bacteria exhibit various morphologies and sizes, from rod-shaped species or spirals to spherical cells, therefore illustrating varied mechanisms that guide faithful cell growth and division processes [15]. Despite recent advances, the mechanism of cell division in ovococci, specifically chromosome organization and segregation, correct division site selection, cell wall synthesis, and cytokinesis that maintain cell shape, remains unknown.

The importance of SepF presented in its directly interaction with and regulation on essential division proteins. In our study, the interaction between SepF and FtsZ was confirmed by three ways, such as bacterial two-hybrid assay, GST pull-down assays and BLI analysis.

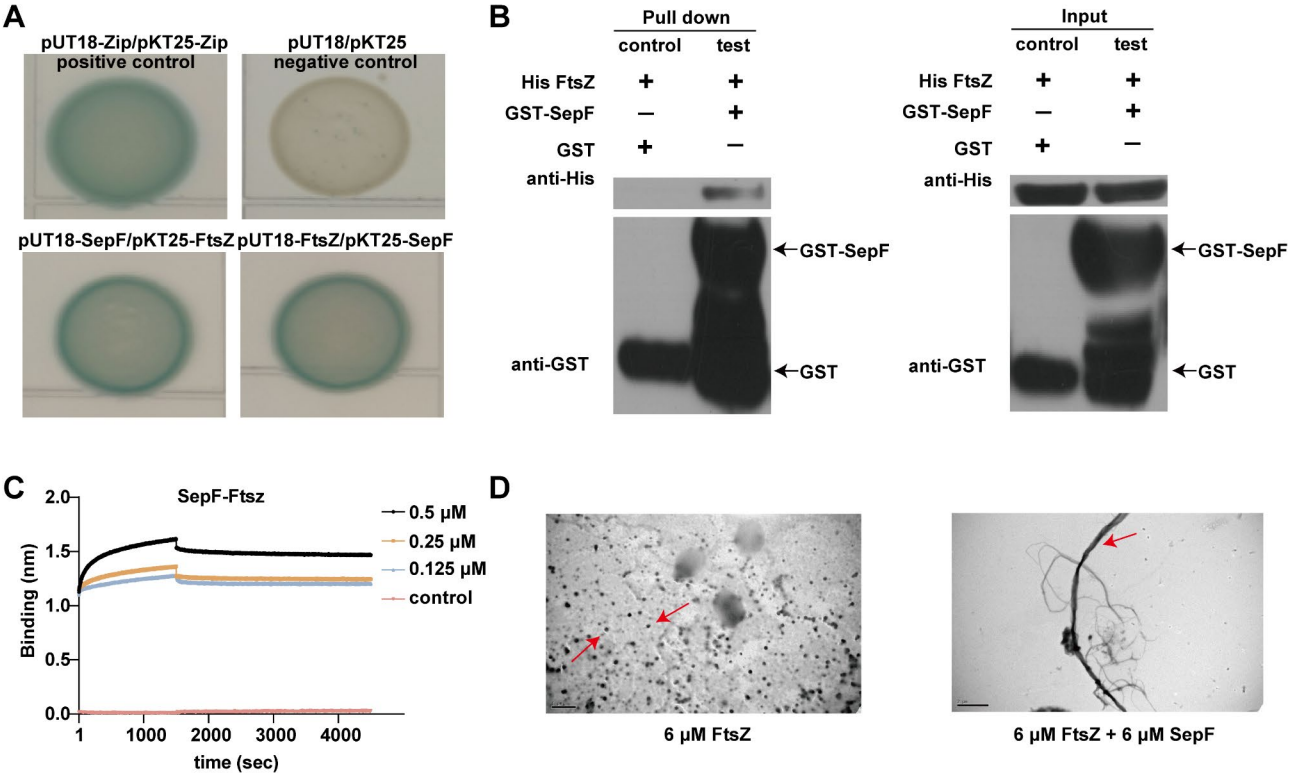

Fig. 4 SepF binded to FtsZ and promoted FtsZ polymerization. **A**: Bacterial two-hybrid assay revealing the interaction between SepF and FtsZ in vivo. pUT-18 and pKT-25 related plasmids were co-transformed into the reporter strain. Positive co-transformants were presented blue dots, while negative co-transformants were presented white dots; **B**: GST pull-down assay revealing the interaction between SepF and FtsZ in vitro. The input channels were used as positive control ($n = 3$ in each group); **C**: BLI assay revealing the interaction between SepF and FtsZ in vitro. The concentration of FtsZ decreased from top to bottom (0.5, 0.25, and 0.125 μM); **D**: SepF enhanced the polymerization of FtsZ. The polymerization reaction of 50 μL was set with a final concentration of 6 μM SepF, 6 μM FtsZ, 1 μM GTP and 10 mM $MgCl_2$ at 30 °C for 15 min. The scale bars are 2 μm

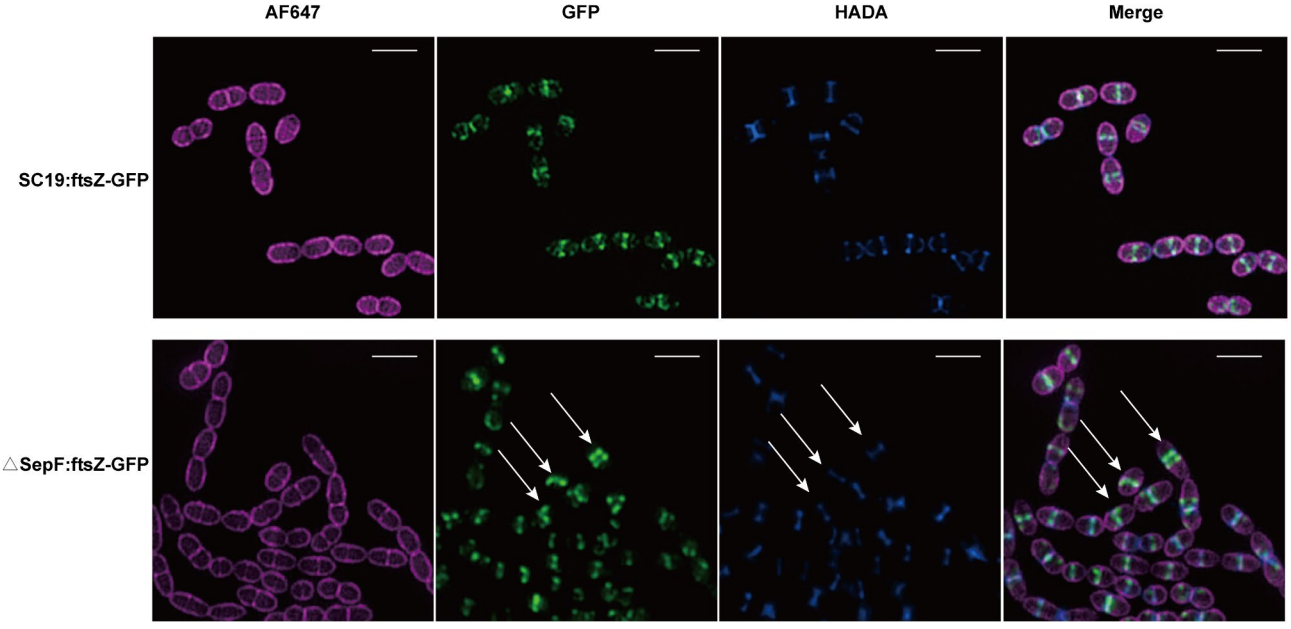

Fig. 5 Structured illumination microscopy analysis of FtsZ-GFP in SC19 and Δ*sepF* strains. The mid-log phase bacterial cells were stained with AF-647 (red fluorescence) and HADA (blue fluorescence) dyes. FtsZ-GFP fusion expression protein presented green fluorescence. White arrow indicated abnormal septums. The scale bars are 2 μm

These methods contain in vivo and in vitro interaction assay. Furthermore, we also found SepF bound to the C-terminal of FtsZ through bacterial two-hybrid (data not shown). The C-terminal domain of FtsZ includes a GTPase-activating site, which requires for FtsZ filamentation and localization [32]. Since FtsZ lacks intrinsic membrane binding ability, it has evolved to interact with the membrane through adaptor proteins that both bind FtsZ and the membrane [33], such as FtsA, SepF, EzrA and ZipA. Consequently, identification the domains or essential amino acids for the interaction between SepF and FtsZ is necessary, especially for drug target discovery in the future.

In previous study, SepF also interacted with MurG, an essential bacterial glycosyltransferase for new septum synthesis to modulate the synthesis of peptidoglycan [13]. In our study, TEM imaget of Δ*sepF* showed abnormal septum which twisted out of shape and disturbed cell division. Because *S. suis* arranged in chain-like conformation that is different from *E. coli* and *M. tuberculosis*. SIM microscopy of green fluorescent protein-tagged FtsZ in *sepF* mutant strain revealed disordered septums that were not organized vertical to the cell long axis and were formed into multiple and un-constricted septums. Our FtsZ localization experiment in *sepF* mutant strains showed that the positioning of FtsZ and its organization in septum structure was dependent on the presence of SepF in the *S. suis* cell. This was also confirmed by the interaction of SepF with FtsZ and the enhancement of its polymerization. Whereas, investigation on SepF from *M. tuberculosis* showed that the positioning of SepF was dependent on FtsZ [34]. Therefore, we speculated that FtsZ and SepF interfered with each other. In previous study, SepF functions as a membrane anchor which brought FtsZ to the division site [35]. However, the assembly hierarchy of SepF and FtsZ is unknown so far.

Conclusion

In conclusion, we reported a SepF homolog from *S. suis*, which deletion was not lethal to *S. suis*. The SepF protein played a vital role in the ovococci divisome and morphogenesis. SepF interacted with FtsZ, inducing filament polymerization. In addition, SepF not only contributed to septum and cell morphology but also regulated SepF via protein-protein interaction. In the further research, we need to know the mechanism of SepF-FtsZ interaction, and identify the binding amino acid site which may be a potential anti-*S. suis* drug target to facilitate drug discovery.

Supplementary Information

The online version contains supplementary material available at https://doi.org/10.1186/s12866-025-03919-3.

Supplementary Material 1

Supplementary Material 2

Supplementary Material 3

Acknowledgements
We would like to thank Wuhan GENECREATE Biological Engineering Co. Ltd. for providing technical support.

Author contributions
Ting Gao, Tingting Li, Linlin Zheng, Mo Chen, Wei Liu, Keli Yang and Jiajia Zhu performed the experiments. Tengfei Zhang, Fangyan Yuan, Zewen Liu and Rui Guo analysed the data. Ting Gao, Danna Zhou and Rui Zhou supervised the study and designed the experiments. Chang Li and Qiong Wu perform the validation. Ting Gao and Jiajia Zhu drafted the manuscript. All authors read and approved the final manuscript.

Funding
This research was supported by the National Key Research and Development Program of China (2021YFD1800401), the Natural Science Foundation of China (NSFC; Grant No. 31802189; 32402901), the Important Science and Technology Project of Hubei Province (2024BBA004), the Technical Innovation Project of Hubei Province (2022ABA002) and the Hubei Province Innovation Center of Agricultural Sciences and Technology (2021-620-000-001-017).

Data availability
All data generated or analyzed during this study are included here and are available from the corresponding author on reasonable request.

Declarations

Consent for publication
Not applicable.

Competing interests
The authors declare no competing interests.

Received: 6 January 2025 / Accepted: 20 March 2025
Published online: 31 March 2025

References

1. Lin L, Xu L, Lv W, Han L, Xiang Y, Fu L, et al. An NLRP3 inflammasome-triggered cytokine storm contributes to Streptococcal toxic shock-like syndrome (STSLS). PLoS Pathog. 2019;15(6):e1007795. https://doi.org/10.1371/journal.ppat.1007795.
2. Wang C, Lu H, Liu M, Wang G, Li X, Lu W, et al. Effective antibacterial and anti-hemolysin activities of ellipticine hydrochloride against Streptococcus suis in a mouse model. Appl Environ Microbiol. 2021;87(10). https://doi.org/10.1128/AEM.03165-20.
3. Lun ZR, Wang QP, Chen XG, Li AX, Zhu XQ. Streptococcus Suis: an emerging zoonotic pathogen. Lancet Infect Dis. 2007;7(3):201–9. https://doi.org/10.1016/S1473-3099(07)70001-4.
4. Yan Z, Pan R, Zhang J, Sun J, Ma X, Dong N, et al. Immunogenicity and protective capacity of sugar ABC transporter Substrate-Binding protein against Streptococcus suis serotype 2, 7 and 9 infection in mice. Vaccines (Basel). 2024;12(5). https://doi.org/10.3390/vaccines12050544.
5. Kuttel MM. Comparative molecular modelling of capsular polysaccharide conformations in Streptococcus suis serotypes 1, 2, 1/2 and 14 identifies common epitopes for antibody binding. Front Mol Biosci. 2022;9:830854. https://doi.org/10.3389/fmolb.2022.830854.
6. Zhu J, Liang Z, Yao H, Wu Z. Identifying Cell-Penetrating peptides for effectively delivering antimicrobial molecules into Streptococcus suis. Antibiot (Basel). 2024;13(8). https://doi.org/10.3390/antibiotics13080725.
7. Tan MF, Tan J, Zeng YB, Li HQ, Yang Q, Zhou R. Antimicrobial resistance phenotypes and genotypes of Streptococcus suis isolated from clinically healthy pigs from 2017 to 2019 in Jiangxi Province, China. J Appl Microbiol. 2021;130(3):797–806. https://doi.org/10.1111/jam.14831.

8. Yongkiettrakul S, Maneerat K, Arechanajan B, Malila Y, Srimanote P, Gottschalk M, Visessanguan W. Antimicrobial susceptibility of Streptococcus suis isolated from diseased pigs, asymptomatic pigs, and human patients in Thailand. BMC Vet Res. 2019;15(1):5. https://doi.org/10.1186/s12917-018-1732-5.
9. Petrocchi-Rilo M, Martinez-Martinez S, Aguaron-Turrientes A, Roca-Martinez E, Garcia-Iglesias MJ, Perez-Fernandez E, et al. Anatomical site, typing, virulence gene profiling, antimicrobial susceptibility and resistance genes of Streptococcus suis isolates recovered from pigs in Spain. Antibiot (Basel). 2021;10(6). https://doi.org/10.3390/antibiotics10060707.
10. Jahan K, Battaje RR, Pratap V, Ahire G, Pushpakaran A, Ashtam A, et al. Identification of ethyl-6-bromo-2((phenylthio)methyl)imidazo[1,2-a]pyridine-3-carboxylate as a narrow spectrum inhibitor of Streptococcus pneumoniae and its FtsZ. Eur J Med Chem. 2024;267:116196. https://doi.org/10.1016/j.ejmech.2024.116196.
11. Pende N, Sogues A, Megrian D, Sartori-Rupp A, England P, Palabikyan H, et al. SepF is the FtsZ anchor in archaea, with features of an ancestral cell division system. Nat Commun. 2021;12(1):3214. https://doi.org/10.1038/s41467-021-23099-8.
12. Hamoen LW, Meile JC, de Jong W, Noirot P, Errington J. SepF, a novel FtsZ-interacting protein required for a late step in cell division. Mol Microbiol. 2006;59(3):989–99. https://doi.org/10.1111/j.1365-2958.2005.04987.x.
13. Zhang H, Chen Y, Zhang Y, Qiao L, Chi X, Han Y, et al. Identification of anti-Mycobacterium tuberculosis agents targeting the interaction of bacterial division proteins FtsZ and SepFe. Acta Pharm Sin B. 2023;13(5):2056–70. https://doi.org/10.1016/j.apsb.2023.01.022.
14. Nussbaum P, Gerstner M, Dingethal M, Erb C, Albers SV. The archaeal protein SepF is essential for cell division in haloferax volcanii. Nat Commun. 2021;12(1):3469. https://doi.org/10.1038/s41467-021-23686-9.
15. Tan MF, Hu Q, Hu Z, Zhang CY, Liu WQ, Gao T, et al. Streptococcus suis MsmK: novel cell division protein interacting with FtsZ and maintaining cell shape. mSphere. 2021;6(2). https://doi.org/10.1128/mSphere.00119-21.
16. Li W, Liu L, Chen H, Zhou R. Identification of Streptococcus suis genes preferentially expressed under iron starvation by selective capture of transcribed sequences. FEMS Microbiol Lett. 2009;292(1):123–33. https://doi.org/10.1111/j.1574-6968.2008.01476.x.
17. Takamatsu D, Osaki M, Sekizaki T. Thermosensitive suicide vectors for gene replacement in Streptococcus suis. Plasmid. 2001;46(2):140–8. https://doi.org/10.1006/plas.2001.1532.
18. Gao T, Yuan F, Liu Z, Liu W, Zhou D, Yang K, et al. MnmE, a central tRNA-Modifying GTPase, is essential for the growth, pathogenicity, and arginine metabolism of Streptococcus suis serotype 2. Front Cell Infect Microbiol. 2019;9:173. https://doi.org/10.3389/fcimb.2019.00173.
19. Hu Q, Yao L, Liao X, Zhang LS, Li HT, Li TT, et al. Comparative phenotypic, proteomic, and phosphoproteomic analysis reveals different roles of serine/threonine phosphatase and kinase in the growth, cell division, and pathogenicity of Streptococcus suis. Microorganisms. 2021;9(12). https://doi.org/10.3390/microorganisms9122442.
20. Gao T, Tan Y, Wang Y, Yuan F, Liu Z, Yang K, et al. Theaflavin ameliorates Streptococcus suis-Induced infection in vitro and in vivo. Int J Mol Sci. 2023;24(8). https://doi.org/10.3390/ijms24087442.
21. Kuru E, Hughes HV, Brown PJ, Hall E, Tekkam S, Cava F, et al. In situ probing of newly synthesized peptidoglycan in live bacteria with fluorescent D-amino acids. Angew Chem Int Ed Engl. 2012;51(50):12519–23. https://doi.org/10.1002/anie.201206749.
22. Jiang Q, Li B, Zhang L, Li T, Hu Q, Li H, et al. DivIVA interacts with the cell wall hydrolase MltG to regulate peptidoglycan synthesis in Streptococcus suis. Microbiol Spectr. 2023;11(3):e0475022. https://doi.org/10.1128/spectrum.04750-22.
23. Zhang H, Feng Y, Si Y, Lu C, Wang J, Wang S, et al. Shank3 ameliorates neuronal injury after cerebral ischemia/reperfusion via inhibiting oxidative stress and inflammation. Redox Biol. 2024;69:102983. https://doi.org/10.1016/j.redox.2023.102983.
24. Liu W, Jiang P, Yang K, Song Q, Yuan F, Liu Z, et al. Mycoplasma hyopneumoniae infection activates the NOD1 signaling pathway to modulate inflammation. Front Cell Infect Microbiol. 2022;12:927840. https://doi.org/10.3389/fcimb.2022.927840.
25. Chakraborty J, Poddar S, Dutta S, Bahulekar V, Harne S, Srinivasan R, Gayathri P. Dynamics of interdomain rotation facilitates FtsZ filament assembly. J Biol Chem. 2024;300(6):107336. https://doi.org/10.1016/j.jbc.2024.107336.
26. Gong H, Yan D, Cui Y, Li Y, Yang J, Yang W, et al. The divisome is a self-enhancing machine in Escherichia coli and caulobacter crescentus. Nat Commun. 2024;15(1):8198. https://doi.org/10.1038/s41467-024-52217-5.
27. Payne IP, Aubry B, Barrows JM, Brown PJB, Goley ED. The cell division protein FzlA performs a conserved function in diverse Alphaproteobacteria. J Bacteriol. 2024;e0022524. https://doi.org/10.1128/jb.00225-24.
28. Massidda O, Novakova L, Vollmer W. From models to pathogens: how much have we learned about Streptococcus pneumoniae cell division? Environ Microbiol. 2013;15(12):3133–57. https://doi.org/10.1111/1462-2920.12189.
29. Halbedel S, Lewis RJ. Structural basis for interaction of DivIVA/GpsB proteins with their ligands. Mol Microbiol. 2019;111(6):1404–15. https://doi.org/10.1111/mmi.14244.
30. Tang J, Guo M, Chen M, Xu B, Ran T, Wang W, et al. A link between STK signalling and capsular polysaccharide synthesis in Streptococcus suis. Nat Commun. 2023;14(1):2480. https://doi.org/10.1038/s41467-023-38210-4.
31. Sha J, Kozlova EV, Fadl AA, Olano JP, Houston CW, Peterson JW, Chopra AK. Molecular characterization of a glucose-inhibited division gene, GidA, that regulates cytotoxic enterotoxin of Aeromonas hydrophila. Infect Immun. 2004;72(2):1084–95. https://doi.org/10.1128/IAI.72.2.1084-1095.2004.
32. Bhattacharya D, King A, McKnight L, Horigian P, Eswara PJ. GpsB interacts with FtsZ in multiple species and May serve as an accessory Z-ring anchor. Mol Biol Cell. 2025;36(1):ar10. https://doi.org/10.1091/mbc.E24-07-0302.
33. Naha A, Haeusser DP, Margolin W, Anchors. A way for FtsZ filaments to stay membrane bound. Mol Microbiol. 2023;120(4):525–38. https://doi.org/10.1111/mmi.15067.
34. Gola S, Munder T, Casonato S, Manganelli R, Vicente M. The essential role of SepF in mycobacterial division. Mol Microbiol. 2015;97(3):560–76. https://doi.org/10.1111/mmi.13050.
35. Gupta S, Banerjee SK, Chatterjee A, Sharma AK, Kundu M, Basu J. Essential protein SepF of mycobacteria interacts with FtsZ and MurG to regulate cell growth and division. Microbiol (Reading). 2015;161(8):1627–38. https://doi.org/10.1099/mic.0.000108.

Publisher's note